Available online at www.sciencedirect.com
ScienceDirect
Journal of Power Sources 176 (2008) 167–174
JOURNAL OF POWER SOURCES
www.elsevier.com/locate/jpowsour

Determination of interfacial adhesion strength between oxide scale and substrate for metallic SOFC interconnects

X. Sun *, W.N. Liu, E. Stephens, M.A. Khaleel

P.O. Box 999, 906 Battelle Boulevard, Pacific Northwest National Laboratory, Richland, WA 99354, United States

Received 4 September 2007; received in revised form 4 October 2007; accepted 5 October 2007
Available online 18 October 2007

Abstract

The interfacial adhesion strength between the oxide scale and the substrate is crucial to the reliability and durability of metallic interconnects in solid oxide fuel cell (SOFC) operating environments. It is necessary, therefore, to establish a methodology to quantify the interfacial adhesion strength between the oxide scale and the metallic interconnect substrate, and furthermore to design and optimize the interconnect material as well as the coating materials to meet the design life of an SOFC system. In this paper, we present an integrated experimental/analytical methodology for quantifying the interfacial adhesion strength between the oxide scale and a ferritic stainless steel interconnect. Stair-stepping indentation tests are used in conjunction with subsequent finite element analyses to predict the interfacial strength between the oxide scale and Crofer 22 APU substrate.

Keywords: Metallic interconnect; Solid oxide fuel cell; Oxide scale; Interfacial strength; Indentation test

1. Introduction

In addition to providing cell-to-cell electrical connections, interconnects in solid oxide fuel cells (SOFCs) also act as separator plates in separating the anode side fuel flow from the cathode side airflow for each cell. Ferritic stainless steel has attracted a great deal of attention for its use as an interconnect in SOFCs because of its gas-tightness, low electrical resistivity, ease of fabrication, and cost-effectiveness. Oxidation reaction of the metallic interconnects in a typical SOFC working environment is unavoidable. Oxide layers generally have high electrical resistivity; therefore interconnect system resistance can be greatly increased by oxide layer thickening. Fig. 1 shows the typical cross-sectional microstructure of Crofer 22 APU after oxidation at 800 °C for 1200 h [1]. Various coating techniques have been proposed and examined in an attempt to protect the ferritic stainless steel interconnect under SOFC operating conditions [1–3], and they have shown great potential in slowing down the oxide scale growth kinetics for various alloys. Even so, sub-coating oxide scale growth is still inevitable.

The growth stresses in the oxide scale and on the scale/substrate interface combined with the thermal stresses induced by thermal expansion coefficient mismatch between the oxide scale and the substrate may lead to scale delamination/buckling and eventual spallation during stack cooling [2,3], which can lead to serious cell performance degradation [4]. Hence, the interfacial adhesion strength between the oxide scale and substrate is crucial to the reliability and durability of the metallic interconnect in SOFC operating environments. It is necessary to establish a methodology to quantify the interfacial adhesion strength between the oxide scale and the metallic interconnect substrate, and to furthermore design and optimize the interconnect material as well as the coating systems to meet the design life of an SOFC system. In this paper, we present an integrated experimental/analytical methodology for quantifying the interfacial adhesion strength between oxide scale and metallic interconnect. Predicted oxide scale adhesion strength for Crofer 22 APU will be discussed.

Micro-indentation tests have been used by various researchers in measuring interfacial properties between coatings and substrates [5–9]. Depending on the type of material systems and indenter shapes, the fundamental mechanics for these measurement approaches can be drastically different. For example, Drory and Hutchinson used indentation tests with a sharp-tip

* Corresponding author. Tel.: +1 509 372 6489; fax: +1 509 375 2604.
E-mail address: xin.sun@pnl.gov (X. Sun).

0378-7753/$ – see front matter © 2007 Elsevier B.V. All rights reserved.
doi:10.1016/j.jpowsour.2007.10.027

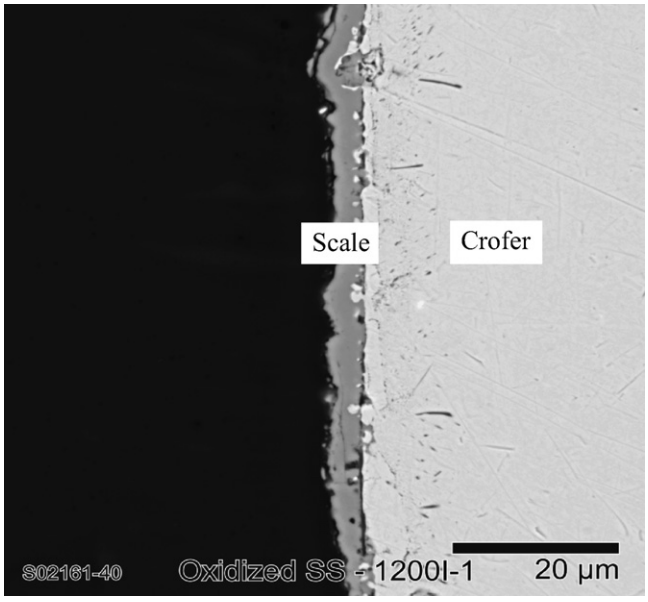

Fig. 1. Cross-sectional microstructures of Crofer 22 APU after oxidation at 800 °C for 1200 h [1].

indenter in measuring the interfacial toughness for brittle coating systems on ductile substrates [5,6]. They deeply penetrated the indenter through the coating film and well into the ductile base metal, creating a large plastic deformation zone in the substrate underneath the indenter tip and around the contact area. Initial crack growth and delamination were not explicitly studied and the most attention was paid to the subsequent interfacial crack growth and delamination propagation process. Mechanics-based solutions were proposed to assess the interfacial toughness from measurements of the applied load, delamination radius, film thickness and film-substrate material properties. Using similar methods, Vasinonta and Beuth [7] measured interfacial toughness in thermal barrier coating (TBC) systems for a gas turbine application. They used the same essential equations proposed by Drory and Hutchinson [5,6] and made necessary modifications to account for the multi-layered TBC systems with effective properties and effective residual strains in the multi-layered system. The interfacial fracture toughness was again calculated with the normalized delaminating radii for various exposure times. Later, Dhanaraj et al. [8] applied similar methodology in measuring the fracture toughness of chromia/substrate interfaces for SOFC interconnect material. In the indentation test, the chromia scale is penetrated by the sharp Brale-C indenter, and the interfacial toughness was then determined from the results of mechanics analysis of the indentation problem and measurement of the delamination radius.

It should be mentioned that, while being an effective method in comparing the bond quality for various coating systems, the fracture toughness-based approach described above has difficulties in predicting cooling-induced oxide/substrate interfacial failure for the SOFC interconnect materials. This is because quantification of energy release rate at the oxide/substrate interface involves fracture mechanics simulations with pre-existing interfacial cracks and very fine mesh. Furthermore, the calculated energy release rate depends on the size, shape, and location of the initial interfacial crack. However, due to the ceramic nature of the chromia scale, random interfacial flaws will be present in the scale and on the oxide scale/substrate interface, making it difficult to determine the actual energy release rate experienced at the interface during cooling.

As an alternative to the interfacial fracture toughness approach, Ritter et al. [9] used a critical shear strength approach in measuring the adhesion of thin polymer coatings to a rigid substrate by indentation. Three types of indentation-induced debonding mechanisms were studied, and the study provided a basis for using a controlled indentation debonding test as a quantitative measure of the interfacial shear strength of thin coatings to rigid substrates.

In this study, we extend the critical shear strength-based approach to quantify the interfacial strength of the brittle oxide and the ductile substrate of SOFC interconnect materials. First, finite element fracture mechanics analyses of micro-indentation tests are performed with pre-existing cracks at the oxide scale/Crofer substrate interface for various crack length, location and scale thickness. It is found that the stress intensity factor in Mode II (i.e., crack surfaces are displaced in a sliding mode) is much higher than that in Mode I (i.e., crack surfaces are displaced in an opening mode) indicating that the interfacial crack tips are mainly shear dominant during indentation. From these results, one can conclude that the interfacial shear stress can be considered as the driving force for interfacial fracture, and that the strength-based failure criterion shares the similar roots as the conventionally used fracture toughness criterion.

The critical interfacial shear strength for an interconnect material candidate (i.e., Crofer 22 APU) is then quantified by an integrated experimental/analytical approach: stair-stepping indentation tests are performed on oxide/substrate systems with various oxide scale thicknesses. The experimentally determined critical indentation forces are then used in conjunction with finite element indentation analyses to determine the critical interfacial shear strength for these various scale thicknesses.

2. Identification of driving force for interfacial delamination of oxide scale and metallic interconnect

In this section, finite element fracture mechanics analyses are used to simulate the indentation test in order to gain more insights on the stress distributions during the indentation test and to identify the driving force for interfacial delamination. A commercial finite element package ABAQUS [10] is used in the fracture mechanics simulation. Fig. 2 shows the schematic of the axisymmetric model for the indentation test. A Brale-C indenter with a 0.2-mm tip radius is used. The indenter tip angle is 120°. Linear elastic material properties are used for both the substrate and the chromia scale. The Young's modulus and Poisson's ratio are 225 MPa and 0.3, respectively for Crofer 22 APU [11,12], and 250 MPa and 0.27, respectively for the chromia scale [13].

A pre-existing interfacial crack with length a is placed on the scale/substrate interface at distance L from the center of the indenter. The typical finite element mesh used in calculating the crack tip stress intensity factors is shown in Fig. 3 which

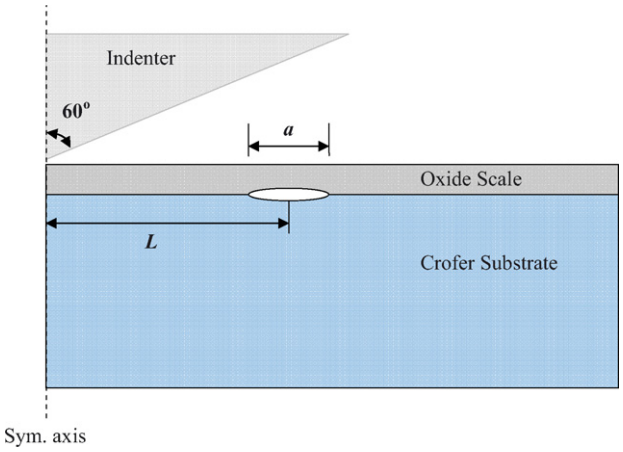

Fig. 2. Schematic of interfacial pre-crack.

consists of 4850 four-node axisymmetric elements and 5005 nodes. Refined mesh is used at the crack tips to ensure accurate stress intensity factor calculations. The detailed finite element mesh zoomed into the crack tip region is also shown in Fig. 3. The left crack tip is denoted as L-tip and the right crack tip is denoted as R-tip. The two regions with different mesh densities are joined together by tying the contact surfaces of the neighboring zones. No penetration contact surfaces are set up between the rigid indenter and the oxide scale surface as well as between the two free surfaces of the crack. Finite element fracture mechanics analyses are then performed for scale thicknesses ranging from 2 to 15 μm and for different crack sizes and initial locations on the interface.

In linear elastic fracture mechanics, crack propagation can be characterized into three modes:

(a) Mode I—opening mode driven by tensile stress normal to the plane of the crack;
(b) Mode II—sliding mode driven by shear stress acting parallel to the plane of the crack and perpendicular to the crack front;
(c) Mode III—out-of-plane tearing mode driven by shear stress acting parallel to the plane of the crack and parallel to the crack front.

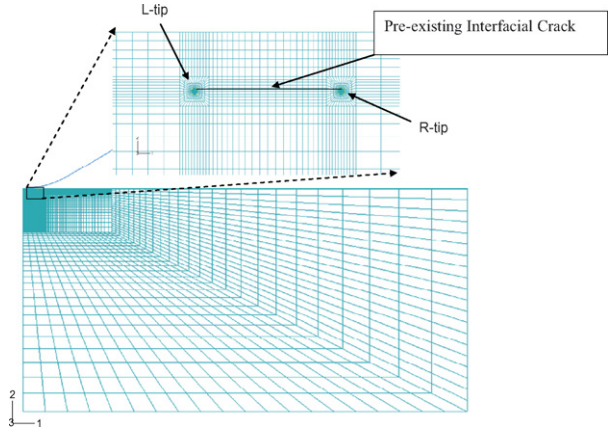

Fig. 3. Typical finite element mesh used in the fracture mechanics analysis.

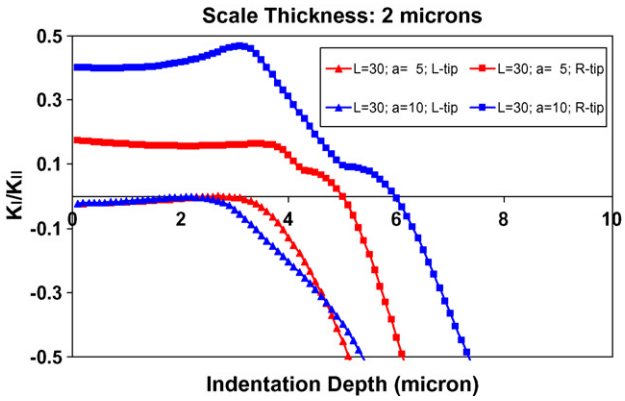

Fig. 4. K_I/K_{II} during indentation test: scale thickness of 2 μm.

At the tip of the crack, a mathematical stress singularity occurs which is characterized by the stress intensity factor K. The stress intensity factor can be quantified separately as K_I corresponding to the opening mode; K_{II} corresponding to the in-plane shear mode; K_{III} corresponding to the out-of-plane tearing mode. In calculating the stress intensity factors at the crack tip, ABAQUS first evaluates the crack tip energy release rate based on the virtual crack extension/domain integral methods. The stress intensity factors for different modes are then extracted using an interaction integral method [10].

Figs. 4–6 illustrate the ratios of the calculated stress intensity factors (i.e., K_I/K_{II}) over the entire indentation depth of 10 μm for scale thicknesses of 2 μm, 5 μm and 15 μm. For each scale thickness, two initial crack lengths are considered: 5 μm and 10 μm. The values of K_I/K_{II} are plotted for both the left crack tip (L-tip) as well as the right crack tip (R-tip). Negative K_I/K_{II} indicates crack closure. In general, for all the cases considered, the results in Figs. 4–6 indicate that the interfacial crack tips have much higher K_{II} than K_I during indentation. In other words, the interfacial crack tips are mostly Mode II dominant. This is true for both the left and the right crack tips. It is also interesting to note that Mode I contribution increases when the crack tip is further away from the center of the indenter (i.e., the right crack tips and the longer cracks). This is particularly true for thinner scales. This is consistent with the typical mixed-

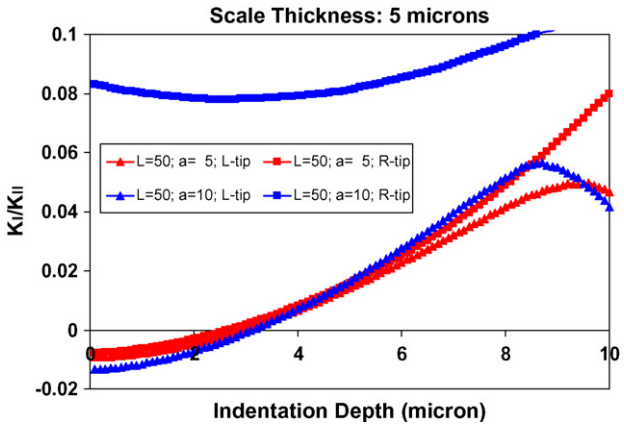

Fig. 5. K_I/K_{II} during indentation test: scale thickness of 5 μm.

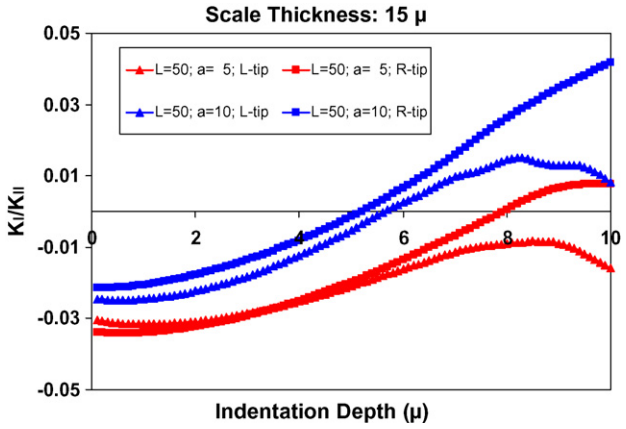

Fig. 6. K_I/K_{II} during indentation test: scale thickness of 15 μm.

mode nature for surface cracks in a Herzian indentation field [14].

Fig. 7 shows the stress intensity factor values versus indentation depth for the interfacial crack of 5 μm length located at 50 μm away from the indenter center. The oxide scale thickness considered is 5 μm. Note that, K_{II} and K_I are plotted on different scales. Clearly, the magnitude of K_{II} is much higher than that of K_I.

By correlating the Mode II dominance of the interface crack tips to the high shear stress observed at the oxide/substrate interface during indentation [9,15], one can now identify shear stress at the interface as the driving force of the failure. At the critical shear stress (i.e., interfacial shear strength), an interfacial fracture will be triggered on the oxide/substrate interface.

3. Experimental stair-stepping indentation test

Room temperature indentation tests were performed on oxidized, bare Crofer 22 APU specimens in quantifying the interfacial strength between the oxide scale and the substrates. A hardness tester was used to apply the load utilizing a Rockwell 1.5875 mm (1/16 in.)-diameter ball indenter to penetrate

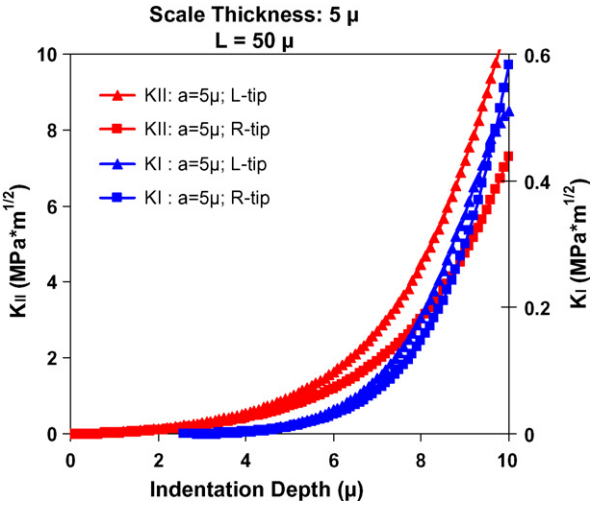

Fig. 7. K_I and K_{II} vs. indentation depth for scale thickness of 5 μm.

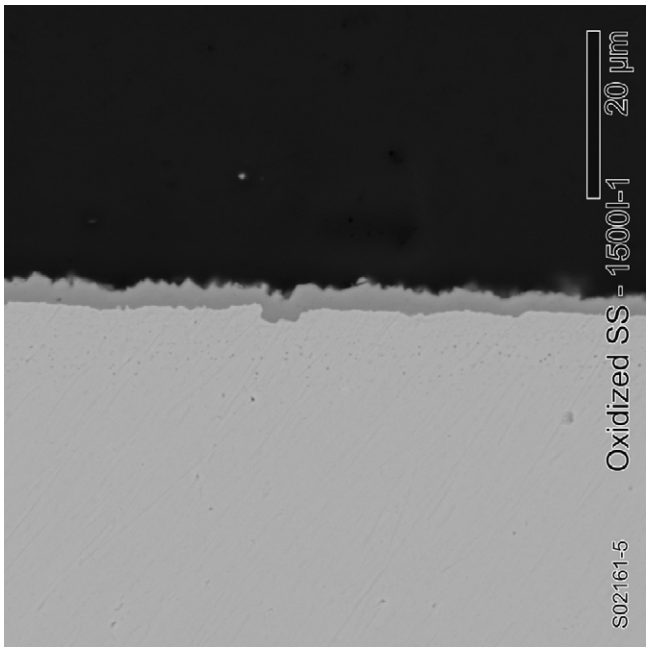

Fig. 8. SEM image representative of the oxide scale observed on the Crofer specimens. A 1500 h oxidized specimen with a measured scale thickness of 2.41 μm is shown.

the oxide scale on the substrates. The loads were stair-stepped between 60 kgf and 150 kgf to determine the critical level that spallation occurred on each specimen. When delamination and spallation were observed, the load was typically reduced and the indentation repeated, continually increasing the load with each indent until failure was observed again.

Seven Crofer specimens oxidized at varying lengths of time were tested. All specimens were oxidized at 800 °C. Metallography was performed to determine the oxide scale thickness for each specimen. Fig. 8 is a scanning electron microscopy (SEM) image representative of the oxide scale observed on the specimens. This particular image is a 1500-h oxidized Crofer specimen with a measured scale thickness of 2.41 μm.

Fig. 9 shows the images representative of typical indentation results observed on an oxidized Crofer specimen with an oxide scale thickness of 2.96 μm. After indentation test at each load level, visual inspection was performed to determine whether a spallation occurred under a microscope. Fig. 10 illustrates the typical failures observed in specimens with a thin oxide scale versus a thicker oxide scale. Typically, in the specimens with a thicker scale layer, a full radial debonding of the scale was observed whereas in specimens with a thinner oxide scale, only localized partial flaking was observed. Fig. 11 shows a cross-sectional view of an indent and the debonding of the oxide scale around the indentation radius.

Table 1 lists the indentation test results. The number of indents that either spalled or did not spall at each load level tested along with the corresponding specimen scale thickness is tabulated. A minimum of two indents for each varying load level was performed on most specimens. Relatively consistent indentation results have been obtained, except for the thinnest oxide thickness where sporadic, partial flaking was observed.

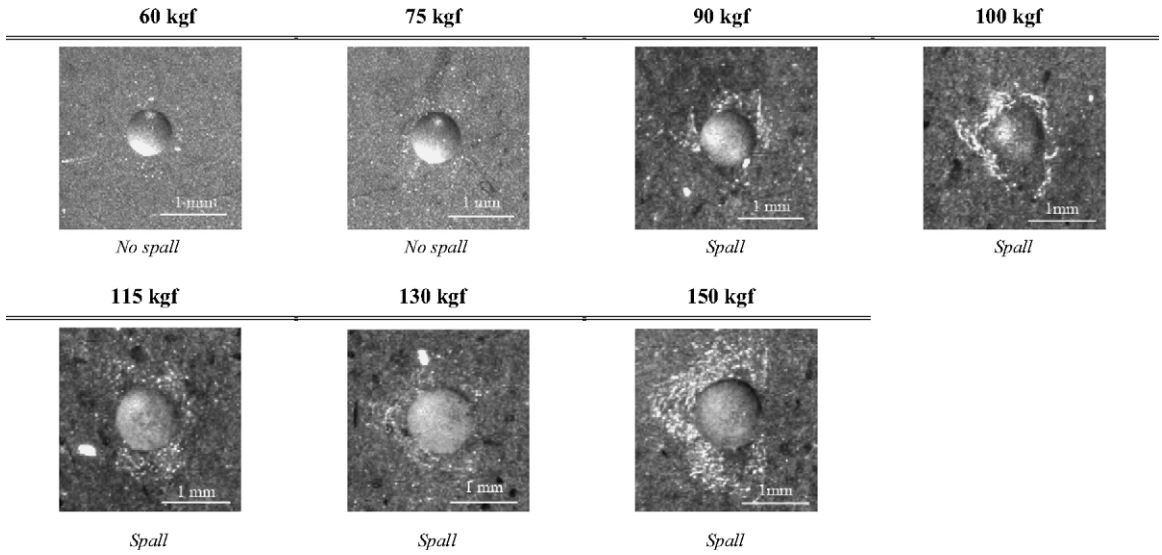

Fig. 9. Images representative of typical indentation results observed on an oxidized Crofer specimen with and without spallation at various test loads. Results shown are from a specimen with an oxide scale thickness of 2.96 μm.

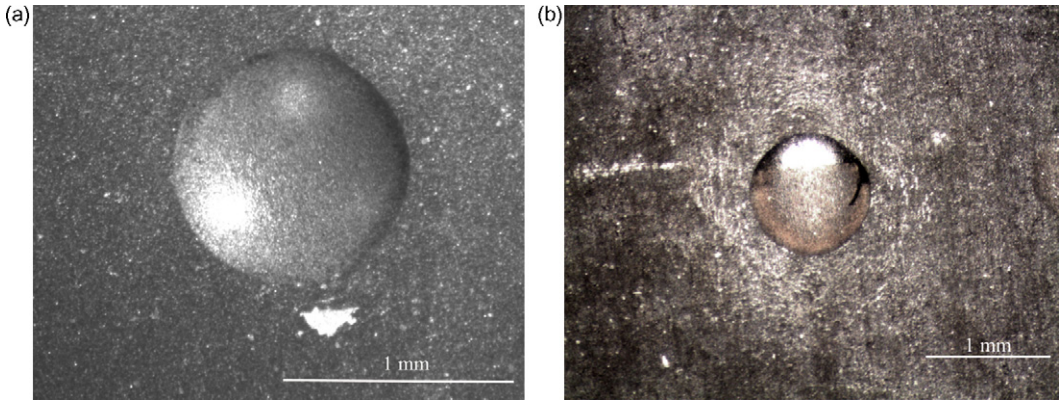

Fig. 10. Photos representative of the spallation observed among the specimens tested. Top views of the indent are shown. Image (a) is an indent tested at 150 kgf on a Crofer specimen with a 1.38 μm thick scale. Image (b) is also an indent tested at 150 kgf; however, on a Crofer specimen with a 2.41 μm thick scale.

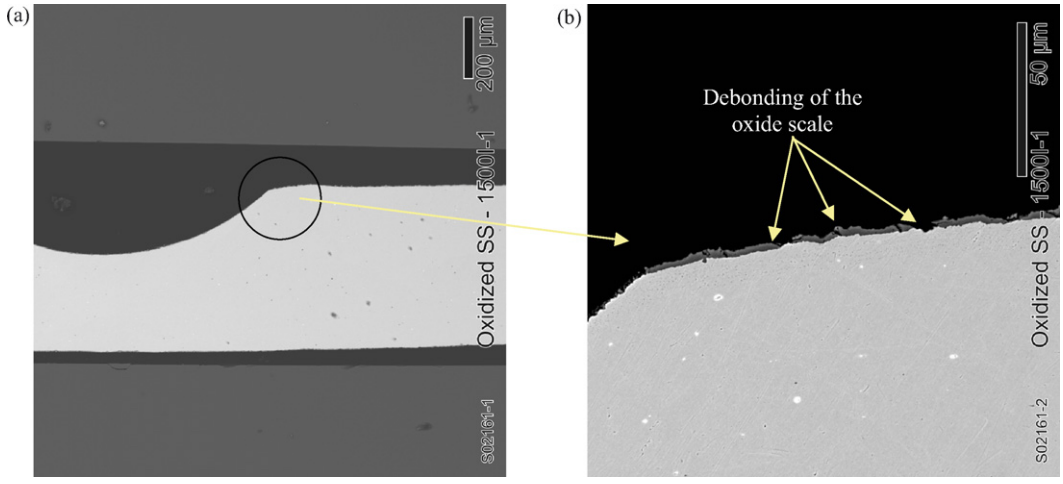

Fig. 11. A cross-sectional view of an indent conducted at 150 kgf (a) and a higher magnification view of the area near the contact radius (b) to observe the debonding of the oxide scale.

Table 1
Indentation test results on oxidized bare Crofer 22 APU with 1/16 in.-diameter Rockwell ball indenter

Spec. #	Scale thickness (μm)	Load (kgf)													
		60		75		90		100		115		130		150	
		No Spall	Spall	No Spall	Spall	No Spall	Spall	No Spall	Spall	No Spall	Spall	No Spall	Spall	No Spall	Spall
1	1.38	2		2		1	1	3		2	1	2		2	1
2	1.50	3		3		3		3		2		3		3	
3	2.04	2		2		2		2		2		2		2	
4	2.06	1		1		1		1		2		2	1	2	
5	2.41	2		2		2		1	1		2		2		2
6	2.71	3		3		3		2	1	2	1	1	2	1	2
7	2.96	3		2		1	1	1	2	1	1		1		2

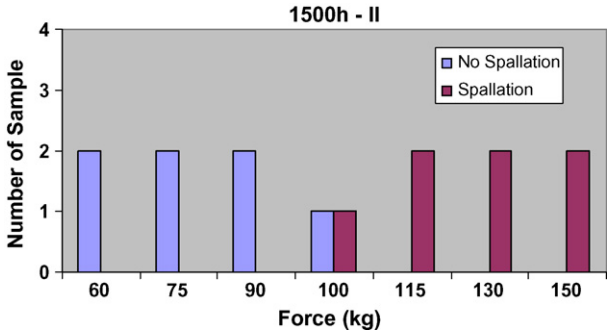

Fig. 12. Illustration of number of failure example during indentation test.

At a particular scale thickness, the number of spalled samples increases with indentation load. On the other hand, under a specific indentation load, more spalled samples are observed with increasing oxide scale thickness. Generally speaking, the results are quite consistent considering the statistical nature of the base metal surface finish, oxide layer thickness as well as pre-existing flaws on the interface.

Fig. 12 illustrates the indentation test results showing the numbers of non-spalled samples and spalled samples with increasing indentation load for the sample with 2.41 μm scale. The sample was oxidized at 800 °C for 1500 h. Clearly, with the resolution of the indentation load used, the critical indentation force to induce scale spallation is 100 kgf. Using similar methods, the critical indentation force for other scale thickness can be obtained. The results are listed in Table 2 for the cases with consistent full-radial debonding. The experimentally determined critical indentation loads for various oxide scale thicknesses will next be inputted into the corresponding finite element indentation model to determine the interfacial shear strength of the interface.

4. Quantification of interfacial shear strength using finite element analysis

Finite element simulations of the Rockwell 1/16 in.-diameter ball indentation tests are performed on the oxide/substrate systems with different oxide thicknesses as listed in Table 2. Fig. 13 illustrates the typical finite element mesh used. Again, a commercial finite element package, ABAQUS [10], is used for the static indentation simulation. The corresponding critical indentation forces are used as input to quantify the interfacial shear strength at spallation for different scale thickness.

Similar analysis procedures as previously described are used except that no pre-existing interfacial crack is present. The characteristic mesh size at the location for maximum shear

Table 2
Critical indentation force observed for different scale thicknesses

Scale thickness (μm)	2.06	2.41	2.71	2.96
Critical indentation force (kgf)	130	100	100	90
Predicted interfacial shear strength (MPa)	454	455	438	423

Mean of predicted interfacial shear strength: 442.5 MPa; standard deviation of predicted interfacial shear strength: 15.2 MPa.

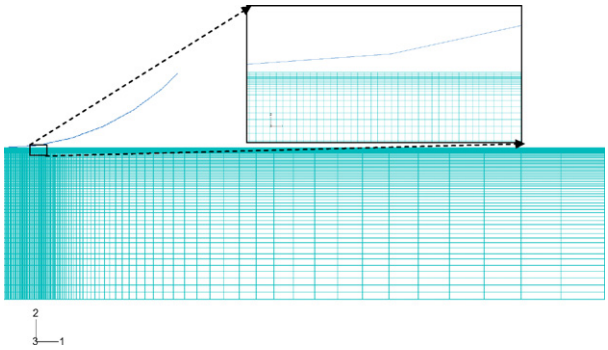

Fig. 13. Finite element mesh used in simulating the Rockwell 1/16 in.-diameter ball indentation test.

stress is around 3 μm. Crofer 22 APU substrate is considered to be elastic–plastic-based on the properties from ThyssenKrupp [11,12]. This is also based on the observed permanent deformation on the indented samples. The chromia scale is again considered as linear elastic with the same properties as previously discussed.

Fig. 14 shows the predicted shear stress contour near the contact radius for the case with 2.41 μm scale at 100 kgf indentation force. The maximum interfacial shear stress occurs around the periphery of the contact radius, consistent with the results presented by Ritter et al. [9]. Note that the σ_{12} contour shown here is under global coordinate only, and the shear stress along the interface should be calculated for each material point on the interface using appropriate coordinate transformations.

Fig. 15 shows the evolution of maximum interfacial shear stress versus indentation force for 2.41 μm oxide scale. The maximum interfacial shear stress corresponding to the critical indentation force of 100 kgf is 455 MPa. Therefore, the stress-based interfacial shear strength is quantified as 455 MPa at the oxide scale/substrate interface.

Following similar analyses procedures, critical interfacial shear strength can be quantified for the indentation tests performed on other scale thickness. The corresponding interfacial strength values predicted are tabulated in Table 2. Given the uneven nature of the oxide scale thickness and morphology as evidenced in Figs. 1 and 9, the predicted interfacial shear strength

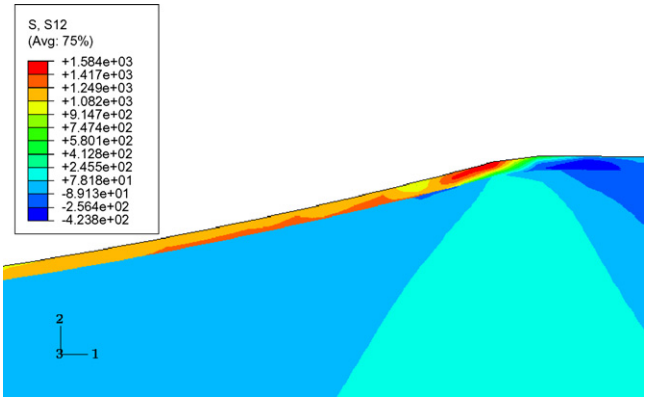

Fig. 14. Predicted contour of shear stress distribution (in global coordinate system) for the scale/Crofer system.

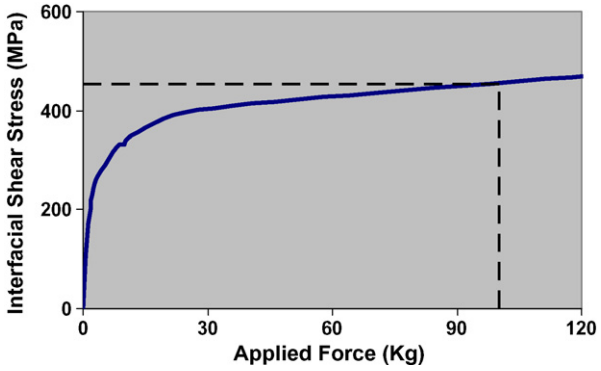

Fig. 15. Maximum interfacial shear stress vs. applied force for 2.41 μm oxide scale.

is quite consistent with the ratio of standard deviation/mean equal to 3.4%.

Besides the statistical nature, it is also interesting to note that the predicted interfacial strength decreases with increasing scale thickness. If this trend is physically true, it indicates a degradation of interfacial strength with increasing oxide scale thickness, which in turn suggests a degradation of interfacial strength with increasing exposure and oxidation time. This can then be related to the growing interfacial residual stress resulted from oxide growth. Future studies with more samples are needed in this area to clarify and quantify the role of growth stress in the stability of oxide/scale adhesion strength during long-term exposure and oxidation.

As discussed by Drory and Hutchinson [6] and Ritter et al [9], different interfacial debonding mechanisms can be invoked using different indenter tips. The goal of our current study is to show that with a standard Rockwell hardness test, oxide/substrate interfacial shear strength can be quantified. The methodology can be used to quantitatively compare the adhesion strength between oxide scale to various candidate interconnect substrate materials. Combined with oxide growth kinetics data, the measured/predicted interfacial strength can also be used to predict the interconnect life under typical SOFC operating conditions [16].

5. Discussions and conclusions

In this paper, we first use finite element fracture mechanics analysis to correlate the Mode II dominance of interfacial crack tip to the high shear stress levels at the interface between oxide/substrate during indentation process. Interfacial shear stress is then identified as the driving force for interfacial delamination between the oxide scale and metallic substrate for SOFC interconnects. A simple, critical shear stress-based interfacial failure criterion is subsequently proposed.

The critical shear strength of the oxide/substrate interface is then quantified using a combined experimental/analytical approach. Stair-stepping indentation tests are performed on oxidized Crofer 22 APU samples to quantify the critical indentation loads at which scale spallation occurs for various scale thickness. Corresponding finite element indentation simulations are then performed to calculate the interfacial shear strength at crit-

ical indentation load. Given the statistical nature of the oxide scale thickness and morphology, relatively consistent adhesion strength has been predicted with small standard deviations. The predicted interfacial strength also indicates some degradation with growing scale thickness. The physical implications and the validity of this observation are subject to future studies.

It should be mentioned that the proposed approach is a deterministic approach and it does not consider the statistical nature of the oxide thickness as well as the interfacial flaw size and distribution. More indentation tests are needed in order to quantify the statistical distribution of the interfacial strength. In addition, the stair-stepping indentation tests and the corresponding finite element indentation simulations are all performed under room temperature. Therefore, high-temperature interfacial strength quantification remains to be the subject for our future study.

Acknowledgements

The Pacific Northwest National Laboratory is operated by Battelle Memorial Institute for the United States Department of Energy under Contract DE-AC06-76RL01830. The work was funded as part of the Solid-State Energy Conversion Alliance (SECA) Core Technology Program by the U.S. Department of Energy's National Energy Technology Laboratory (NETL). We would like to acknowledge the technical discussions and directions from Wayne Surdoval, Travis Shultz and Lane Wilson.

References

[1] J.W. Fergus, Mater. Sci. Eng. A (Struct. Mater.: Prop. Microstruct. Process.) 397 (1–2) (2005) 271–283.
[2] Z. Yang, G. Xia, J.W. Stevenson, Electrochem. Solid State Lett. 8 (3) (2005) 168–170.
[3] Z. Yang, J.S. Hardy, M.S. Walker, G. Xia, S.P. Simner, J.W. Stevenson, J. Electrochem. Soc. 151 (11) (2004) A1825–A1831.
[4] J.Y. Kim, V.L. Sprenkle, N.L. Canfield, K.D. Meinhardt, L.A. Chick, J. Electrochem. Soc. 153 (5) (2006) A880–A886.
[5] M.D. Drory, J.W. Hutchinson, Proc. Roy. Soc. London 452 (1996) 2319.
[6] M.D. Drory, J.W. Hutchinson, Mater. Res. Soc. Symp. Proc. 383 (1995) 173–182.
[7] A. Vasinonta, J.L. Beuth, Eng. Fract. Mech. 68 (2001) 843–860.
[8] N. Dhanaraj, J. Beuth, G. Meier, F. Pettit, J. Hammer, S. Laney, Interfacial Fracture Testing to Evaluate the Durability of SOFC Interconnect Alloys, Materials for the Hydrogen Economy, Organized by J.J. Petrovic, I.E. Anderson, T.M. Adams, G. Sandrock, C.F. Legzdins, J.W. Stevenson, Z.G. Yang, Mater. Sci. Technol. 2005 pp. 165–175.
[9] J.E. Ritter, T.J. Lardner, L. Rosenfeld, M.R. Lin, J. Appl. Phys. 66 (8) (1989) 3626–3634.
[10] ABAQUS/Standard User's Manual, Hibbitt, Karlsson and Sorensen Inc., 2002.
[11] Material Data Sheet no. 4046: Crofer 22 APU, July 2005, ThyssenKrupp VDM.
[12] Young's modulus of Crofer 22 APU, January 2006, ThyssenKrupp VDM.
[13] A.M. Huntz, Mater. Sci. Eng. A201 (1995) 211–228.
[14] X. Sun, M.A. Khaleel, Proceedings of the 31st International Conference on Advanced Ceramics and Composites, ICPSS-257519, January 21–26, 2007.
[15] X. Sun, W.N. Liu, P. Singh, M.A. Khaleel, Effects of Oxide Thickness on Scale and Interface Stresses under Isothermal Cooling and Micro-Indentation, PNNL Report 15794, Pacific Northwest National Laboratory, Richland, WA, May 2006.
[16] X. Sun, W.N. Liu, E. Stephens and M.A. Khaleel, Interfacial Strength and IC Life Quantification using an Integrated Experimental/Modeling Approach, PNNL Report 16610, Pacific Northwest National Laboratory, Richland, WA, May 2007.